Biochimica et Biophysica Acta 1823 (2012) 1406–1415

Contents lists available at SciVerse ScienceDirect

Biochimica et Biophysica Acta

journal homepage: www.elsevier.com/locate/bbamcr

Review

Visualizing metal ions in cells: An overview of analytical techniques, approaches, and probes ☆

Kevin M. Dean, Yan Qin, Amy E. Palmer *

ARTICLE INFO

Article history:
Received 6 February 2012
Received in revised form 2 April 2012
Accepted 3 April 2012
Available online 13 April 2012

Keywords:
Metal ion homeostasis
Fluorescence imaging
Fluorescent sensors
Imaging metal ions in cells

ABSTRACT

Quantifying the amount and defining the location of metal ions in cells and organisms are critical steps in understanding metal homeostasis and how dyshomeostasis causes or is a consequence of disease. A number of recent advances have been made in the development and application of analytical methods to visualize metal ions in biological specimens. Here, we briefly summarize these advances before focusing in more depth on probes for examining transition metals in living cells with high spatial and temporal resolution using fluorescence microscopy. This article is part of a Special Issue entitled: Cell Biology of Metals.

© 2012 Elsevier B.V. All rights reserved.

1. Introduction

Metal ions play fundamental roles in biology by serving as essential cofactors in processes such as respiration, growth, gene transcription, enzymatic reactions, cell proliferation and immune function. These essential metals can also be toxic at elevated levels and therefore metal import, trafficking, availability and export must be tightly regulated at the cellular level. Collectively, these processes are referred to as homeostasis. Not surprisingly, altered metal homeostasis is associated with a wide array of primary pathologies and diseases including genetic disorders, degenerative diseases, cancer, and diabetes [1–5]. Metal homeostasis can also be altered secondary to other diseases and treatments [6]. For example, hemochromatosis (i.e. iron overload) can occur due to frequent blood transfusions [7], and zinc deficiency due to chronic liver disease or intestinal malabsorption [8,9]. As evidenced by the other articles in this special issue, the scientific community has amassed substantial mechanistic details of how metal ions can be used as cofactors in biomolecules and is making significant progress toward building a picture of the molecular players involved in metal homeostasis. Despite these advances, we know far less about the subcellular location, speciation, and dynamics of metal ions. With the development of tools and techniques for mapping metal ions in both fixed and living cells, we are beginning to reveal how metals are distributed in cells.

Transition metals can exist in many different forms within cells, including free ions,[1] bound to biomolecules such as proteins, or in association with low molecular weight species such as amino acids or glutathione, from which the metal ion could be released by changes in the cellular environment. Given the role of many metal ions as catalytic cofactors or structural stabilizers in enzymes and proteins, it is widely accepted that a substantial amount of the cellular metal ion pool is bound to enzymes, proteins, and other low molecular weight species. As a consequence, these intracellular components buffer the amount of free metal that is thermodynamically and kinetically accessible [10]. While it is relatively straightforward to determine the total metal content of a cell using techniques such as atomic absorption spectroscopy or inductively coupled plasma mass spectrometry, it is much more challenging to define where metals are located and what chemical form they are in (i.e. their speciation[2]). Yet mapping metals in cellular sub-compartments within the cell is a necessary step in understanding metal homeostasis.

Several lines of evidence suggest metal ions are unlikely to be evenly distributed throughout a cell. First and foremost, imaging techniques have yielded images of uneven distribution of metals in cells [11,12]. Secondly, there is evidence, at least in bacteria, that cells exploit compartmentalization to buffer metal ions at different levels in different locations (e.g. cytosol versus periplasm) as one mechanism of ensuring the correct metal is loaded into the correct protein [13,14]. Lastly, a vast array of channels, carriers, and pumps exhibit tissue-specific patterns of localization across cells and sub-

☆ This article is part of a Special Issue entitled: Cell Biology of Metals.

* Corresponding author at: UCB 596, Department of Chemistry and Biochemistry and BioFrontiers Institute, University of Colorado, Boulder, CO 80309, United States. Tel.: +1 303 492 1945.
E-mail address: amy.palmer@colorado.edu (A.E. Palmer).

[1] Free ion is not meant to mean that the metal ion is completely stripped of bound ligands. It is assumed that in the aqueous cellular environment, the metal ion is likely to be bound by water or other ionic ligands.

[2] This could include differences in oxidation state, free versus bound, or even the nature of bound species.

0167-4889/$ – see front matter © 2012 Elsevier B.V. All rights reserved.
doi:10.1016/j.bbamcr.2012.04.001

cellular compartments, supporting the notion that metal concentrations are likely to be different in different regions within a cell [15–17].

To complicate matters even further, emerging evidence suggests that metal ions can be mobilized from labile pools in cells [18], suggesting that in addition to spatial heterogeneity, there is an important temporal component that is likely influenced by specific cellular events. The idea that transient changes in metal ion concentrations may lead to the generation of metal ion "signals" represents an exciting paradigm for investigating how cells control levels of metal ions and how metal ions influence cellular function. Exploring these parameters requires analytical tools and techniques to define metal content with high spatial and temporal resolution. This has led to significant advances in recent years in the ability to map metals in cells, including the application of analytical techniques as well as the development of novel probes. This article will briefly summarize the different analytical techniques, as well as review the main classes of probes, their capabilities (strengths and weaknesses), and emphasize exciting new discoveries made possible by these probes. Because the majority of these probes have been applied to mammalian cells, this review will focus on these systems. However, it is important to point out that these tools may be compatible with other biological systems including bacteria, yeast, plants, and others.

2. Analytical techniques for imaging metal ions in biology

A variety of techniques have been developed and used to visualize specific metal ions in biological samples in a way that preserves the spatial distribution. This can be done on either fixed or live specimens. A suite of analytical techniques capable of defining metal distribution have been applied to fixed biological specimens, including spatially resolved mass spectrometry techniques [19] such as secondary ion mass spectrometry (SIMS), and laser ablation inductively coupled plasma mass spectrometry (LA-ICP-MS), electron spectroscopy imaging (ESI) combined with electron energy loss spectroscopy (EELS) [20,21], and X-ray fluorescence microscopy (XRFM) [11,22]. Each of these techniques allows researchers to define total metal content (they do not differentiate between "free" and bound metal ions) with high sensitivity and sub-cellular spatial resolution. Of these techniques, XRFM has probably received the most widespread application. This technique involves the use of high flux, hard, X-rays from synchrotron radiation sources that can be focused to a submicron spot and raster scanned across a sample. Irradiation of the sample leads to excitation of a core electron and emission of a photon with a defined energy. Because different elements have different electronic structures, the energy of the emitted photon is characteristic of a particular element and hence the technique permits mapping of multiple elements simultaneously. The above techniques for mapping metal ions in fixed specimens are the focus of several comprehensive recent reviews and will not be considered further [11,19,22]. The remainder of this review will instead highlight recent developments in the application of microscopy techniques for visualizing metal distribution and dynamics in living specimens.

A key component of using microscopy to image metal ions in living cells, tissues, and organisms is the availability of probes that enable visualization of the metal ion of interest. These probes must have a mechanism of converting metal binding into an optical signal that can be measured by the appropriate imaging modality. These optical read-outs could include, but are not limited to, fluorescence, phosphorescence, luminescence, or magnetic resonance imaging (MRI). For imaging at the cellular level, by far the most prevalent mechanism for optical detection is fluorescence [23,24]. Fluorescence is also well-suited for imaging small optically transparent organisms [25], and increasingly for intra-vital imaging as well [26]. Fluorescent sensors typically fall into one of three categories that are differentiated according to how metal binding alters the fluorescence properties. Metal binding could alter the fluorescence intensity (referred to as intensiometric sensors), the wavelength of excitation or emission (ratiometric sensors), or fluorescence lifetime. Fluorescent sensors based on a variety of platforms (small molecule, genetically encoded, etc) have been developed for an array of metal ions and these are highlighted below.

Phosphorescence is related to fluorescence but it is characterized by a long excited state lifetime (e.g., μs) due to the fact that emission of a photon from a triplet excited state to a singlet ground state is a spin-forbidden process [24]. This leads to a longer time delay for emission and this photophysical property can be capitalized on to generate sensors for metal ions based on fluorescence lifetime. Indeed recently the Lippard lab generated the first phosphorescent sensor for Zn^{2+} and used fluorescence lifetime imaging microscopy (FLIM) to monitor increases in Zn^{2+} in human alveolar epithelial A549 cells [27].

Chemiluminescence (or bioluminescence) involves the detection of photons upon reaction of a substrate with an enzyme, such as the oxidation of luciferin by luciferase. Luminescent signals are typically weaker than corresponding fluorescence signals [28], however due to the lack of reliance on excitation light, luminescence benefits from low background, and often gives rise to improved signal to noise [28,29]. Luminescence is a highly advantageous imaging modality for small animals due to its simplicity, ease-of-use, readily available instrumentation, and extreme sensitivity (as few as 100 plaque forming units (pfu) of luciferase expressing virus have been detected *in vivo* [30]). Although luminescence has been exploited to generate sensors for cellular targets, including cAMP [31] and kinase activity [32,33], no chemiluminescent sensors for metal ions have been developed thus far.

Magnetic resonance imaging (MRI) complements the above optical techniques by providing the opportunity to image metal ions in 3D in optically opaque living organisms. MRI signals arise due to modulation of the relaxation properties of the protons of water. So-called "smart" contrast agents give rise to an MRI signal in response to environmental cues, such as sensing of metal ions. Recent review articles highlight advances in the development of metal-responsive MRI contrast agents [34,35].

3. Classes of fluorescent sensors for live cell imaging

When imaging metals in living cells, there are three major fluorescence-based platforms from which one can choose: small-molecule sensors, protein-based biosensors, and hybrid probes that integrate small-molecule sensors with genetically encoded elements (e.g., SNAP-tag [36]). Each system offers its own advantages and disadvantages, including ease of use, dynamic range, brightness, apparent dissociation constant, specificity, and ability to be targeted to specific sub-cellular organelles. In general, no single probe (or class of probes) is likely to be the magic bullet, ideal for addressing the wide array of scientific questions related to quantitative and dynamic imaging of metals in cells. Fig. 1 provides an overview of these classes of probes and gives examples of each type.

Small-molecule indicators, initially pioneered by Tsien and coworkers to detect intracellular Ca^{2+} [37–39], are constructed from a fluorescent moiety (e.g., fluorescein, rhodamine, cyanine) covalently attached to a chelating agent. Mechanistically, many small-molecule probes rely upon photo-induced electron transfer between the fluorescent moiety and the chelating agent to quench fluorescence in the unbound state [40]. Binding of the metal decreases the charge transfer rate, thus improving the quantum-yield of fluorescence, and resulting in an intensity-based output that is related to the sensor dissociation constant and the local metal concentration. As a result of the large differences in quantum yield between the bound and unbound state, as well as more subtle differences in extinction coefficients, this modular design has provided small-molecule probes with impressive dynamic ranges (>150-fold) [41,42]. Furthermore,

alterations in the chelating moiety provide tuning of the specificity and affinity, allowing tuning of the dissociation constants from femtomolar to micromolar concentrations [43,44].

Despite these advantages, small-molecule sensors must be introduced into the intracellular environment in a minimally invasive manner. If the sensor is membrane permeable, this can be accomplished by simply adding sensor into the extracellular media prior to imaging. However, given the charged nature of many chelating agents and fluorophores, electrostatic charge typically renders the sensor membrane impermeable. If the probe permits, partial neutralization of the charge by acetoxymethyl (AM) esters can facilitate translocation across the membrane and restoration of native sensor after cleavage by intracellular esterases [45]. This approach has found widespread usage in several commercially available Ca^{2+} and Zn^{2+} indicators (Fig. 1d). Other strategies include microinjection, covalent or electrostatic attachment of the sensor to cell-penetrating peptides, or analogous to DNA transfection, encapsulation of the sensor in a biologically inert matrix.

An alternative approach is to use genetically encoded protein-based biosensors. These often consist of one or more fluorescent proteins (FP) fused to a naturally occurring or engineered metal binding domain. For single-FP biosensors, binding of the metal triggers a change in fluorescence intensity or wavelength through rearrangements local to the FP chromophore (Fig. 1c). Single-FP sensors, because of their rapid millisecond kinetics and large dynamic range (>100-fold), much like small-molecule sensors, are particularly useful for sensitive detection of small transient signals (e.g., Calcium waves) [46,47]. Multi-FP sensors, which typically consist of two FPs separated by a metal-sensing domain, rely upon Forster Resonance Energy Transfer (FRET) to measure the local concentration of a desired metal (Fig. 1a). Here, binding of a metal ion alters the inter-chromophore distance and/or orientation, thereby altering the rate of energy transfer from the donor (e.g., Cyan FP) to the acceptor (e.g. Yellow FP) fluorophores [48–52]. Unlike intensity-based sensors, both the donor and acceptor fluorescence intensities are measured and the ratio of the two intensities provides a quantitative measure of the metal ion concentration. Nevertheless, the benefit of metal ion quantification comes at the manageable cost of slower response kinetics and decreased dynamic ranges.

Perhaps most importantly, placing the sensor under control of a cell-specific promoter, or fusing the sensor to a particular localization signal sequence, can target single-FP and multi-FP sensors targeted to distinct cell-types within tissues, as well as specific sub-cellular locations within the cell. For example, genetically encoded sensors can be targeted with high fidelity to places where their small-molecule counterparts often face challenges, including the endoplasmic reticulum, Golgi apparatus, and even the pre-synaptic cleft of a hippocampal neuron [53,54]. Additionally, the use of viral gene-transfer techniques allows the system to be expanded to living organisms, a technique that has enabled long-term imaging of neuronal processes [46,55].

Hybrid-probes seek to enable the genetic specificity afforded by FP-based biosensors with the spectral diversity and large dynamic ranges provided by small-molecule probes. For example, the SNAP-

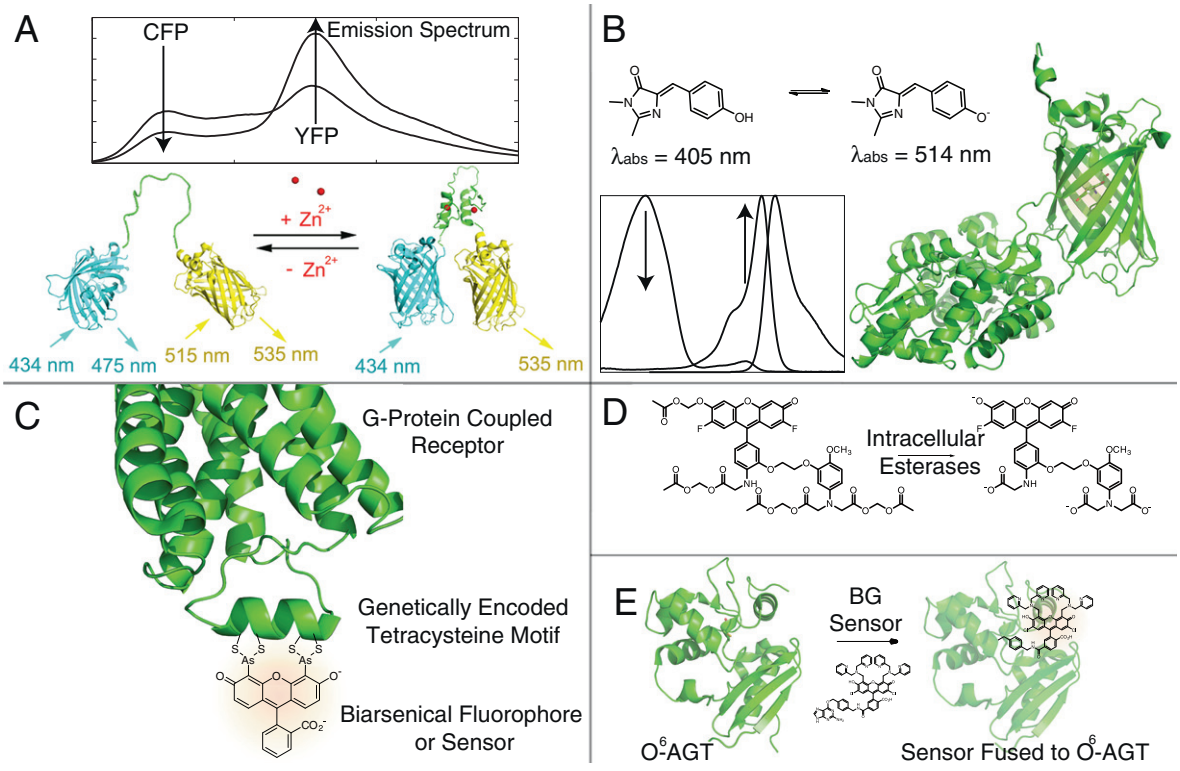

Fig. 1. General mechanisms of live-cell metal sensing. (A) Binding of zinc by a multi-FP sensor changes the conformation and/or distance between the donor fluorophore (CFP) and the acceptor fluorophore (YFP), resulting in a change in the FRET ratio that is proportional to zinc bound. Current probes of this class include ZifCY [48], ZapCY [51], and eCALWY [49] sensors. (B) Ligand binding in a circularly permuted single-FP sensor (PDB 3OSQ) alters the fluorescence intensity of the sensor through changes in the quantum yield and/or extinction coefficient, or the ratio of protonated to deprotonated forms of the chromophore. While this approach has been widely adopted for the development of Ca^{2+} sensors, it has not yet been applied for transition metal ions. (C) Small-molecule biarsenical fluorophore, FlAsH shown, or sensor (e.g., Calcium Green), selectively binds tetracysteine motif engineered on the intracellular loop of a G-protein coupled receptor (PDB 2RH1). (D) Translocation across the plasma membrane is facilitated by masking charges on the small-molecule sensor, FluoZin-3 shown, with acetoxymethyl (AM) esters. Upon exposure to intracellular esterases, the AM-esters are cleaved, exposing charges on the carboxylic acids, and thereby trapping the sensor within the cell [45]. (E) Sub-cellular spatial control over small-molecule sensors is accomplished by genetically targeting O6-Alkylguanine-DNA Alkyltransferase (AGT, aka SNAP-Tag, PDB 3KZY and 3LOO), an enzyme that catalyzes covalent bond formation with a benzylguanine (BG) small-molecule sensor [56].

tag system has been used to provide organelle specificity [56–58]. Here, genetic targeting of O^6-alkylguanine transferase (AGT) provides subcellular localization, which undergoes site-specific cysteine alkylation and covalent labeling by benzylguanine-tethered sensors (Fig. 1e) [36]. Lippard and coworkers used this approach to target their small molecule zinc sensor, ZP1, to the mitochondria and Golgi apparatus in living cells [56]. An alternative strategy includes tethering a sensor to a biarsenical FlAsH motif, which recognizes a specific tetrasysteine peptide in vivo, as was employed to target calcium-green-FlAsH to the a membrane-associated calcium channel (Fig. 1b) [59]. Additionally, phage-display has been used to develop peptides that selectively and with high-affinity bind calcium indicators in vivo [60]. Nevertheless, these systems still suffer to varying extents from non-specific and fluorescent background due to incomplete removal of the sensor, or in the case of FlAsH, palmitoylation or partial oxidation of the biarsenical motif.

Regardless of the metal sensing system one chooses, verifying that the sensor is not perturbing the system under study is paramount. Given the size of fluorescent proteins (≈30 kDa), or the SNAP-tag system (≈20 kDa), it is important to confirm that fusion to endogenous proteins does not alter their function *in vivo*, or perturb vital cellular functions (e.g., cell division). Given that metal ions may be buffered at very low levels, a particular concern is to test whether addition of a sensor alters the concentration of free metal ion. Indeed, a small molecule sensor FluoZin3 was shown to significantly alter resting levels of Zn^{2+} [61], while two genetically encoded platforms did not cause significant perturbation [49,51]. Additionally, the brightness of the sensor, defined as the product of the extinction coefficient and the quantum yield, as well as its excitation wavelength, are important to minimize cellular phototoxicity. For example, longer wavelengths probes are preferable to those excited at UV wavelengths, and brighter probes enable more sensitive detection and shorter image acquisition durations.

The nature of the signal is also important. For intensity-based sensors, a turn-on response is more intuitive and provides improved contrast over turn-off sensors. While for ratiometric sensors, desired features include a large dynamic range, and a wavelength shift between the bound and unbound sensors that is easily separable with commercially available fluorescence filter sets. Naturally, a given sensor should be specific to a particular ion, and insensitive to other active cations at their relevant concentrations. Furthermore, its response to pH should be considered, especially when comparing alkaline (i.e., the cytosol, pH ≈ 7.4) and acidic environments (endocytic vacuole, pH ≈ 4.5). Lastly, the sensor should be insensitive to environmental redox properties.

There are numerous ways to target sensors to sub-cellular compartments, including incorporation of signal sequences, fusion to specific proteins, or for chemical probes, reliance on membrane potential. Fig. 2 highlights the fluorescent indicators for Zn^{2+}, Cu^{1+}, and Fe^{3+} that have been targeted to or are sequestered in different subcellular compartments. For intensity-based small molecule sensors that are sequestered into organelles by chemical moieties (for example the a motif that targets the negative membrane potential of the mitochondria or the low pH of vesicles) it is important to remember that the fluorescence intensity depends both on the dye concentration (how much is sequestered into a given compartment), path-length through the cell (e.g., a thin cytosolic protrusion as opposed to the substantially thicker nucleus), as well as the metal ion concentration (which affects the fluorescence intensity) and to ensure that dye localization is not altered by cellular perturbations such as loss of membrane potential. For example, the negative membrane potential of mitochondria is due to the pH gradient generated by the electron transport chain (aka oxidative phosphorylation). The negative membrane potential can be dissipated by a variety of chemical and biological uncouplers, or increased by ATP synthase inhibitors, such as oligomycin, and such perturbations may also change dye localization.

4. Overview of fluorescent probes for biological metal ions

In recent years, major advances have been made in the development of both small molecule and genetically encoded sensors for Zn^{2+}, Cu^{1+} and Cu^{2+}. Fig. 3 (also see Supporting Information Table 1) presents a summary of the best small molecule sensors, highlighting the excitation wavelength, relative affinity (pK_D), and dynamic range (larger symbols correspond to larger dynamic ranges), while Table 1 presents the corresponding information for genetically encoded probes.

4.1. Fluorescent probes for Zn^{2+}

Design and application of fluorescent probes for imaging labile Zn^{2+} in biological samples can be traced back to late 1960s when it was discovered that zinc could form fluorescent complexes with quinoline [62,63]. The quinoline derivative TSQ (6-methoxy-8-*p*-oluenesulfonamidoquinoline) was successfully used in identifying a pool of free Zn^{2+} in the brain [63]. Later, zinquin, with improved water solubility and cell permeability, was developed to monitor free Zn^{2+} in living cells [64]. However, UV light excitation limited the application of zinquin, as well as other UV-excitable fluorophores for studying Zn^{2+}, due to the damaging effects of UV irradiation to living cells. To address these limitations, a series of non-UV light excitable Zn^{2+} sensors have been developed based on different platforms and these probes have been successfully used for different biological applications. Below, we summarize the main classes and recent developments, and refer readers to several recent reviews [12,65,66] for more detailed information.

As mentioned previously, the most commonly used sensor platform relies upon photoinduced electron transfer (PET) between a fluorophore and its metal-specific chelate. In particular, several research groups have utilized DPA (di-2-picolylamine) as a receptor and the fluorescein as a fluorophore. Examples are Zinpyr (ZP) family [67–69] and Zinspy (ZS) family [70,71] from the Lippard group, Newport Green from Life Technologies (Molecular Probes) [41] and the ZnAF family from Nagano group [72]. By replacing the receptor DPA with quinoline, the Lippard group also developed Quinozin (QZ) family sensors [73]. These sensors demonstrated better photophysical, thermodynamic, and kinetic properties compared to DPA based sensors, yielding greater specificity for Zn^{2+} and a larger dynamic range. Substitution of fluorescein with other fluorophores such as boron dipyrromethene (BODIPY) led to the development of BDA [74] which is red-shifted relative to fluorescein, and impervious to pH changes over a wide range (pH 3–10).

In addition to tuning the fluorophore moiety, researchers have also modified the receptor of well characterized calcium sensors to switch the calcium selectivity to Zn^{2+} selectivity. Removing one or more chelating moieties of bis(*o*-aminophenoxy)-ethane-*N*,*N*,*N*′,*N*′-tetraacetic acid (BAPTA) of fluo-3 and fluo-4, resulted in the creation of FluoZin family sensors with very low affinity for Ca^{2+} [41]. FluoZin3 displays a dissociation constant for Zn^{2+} that is compatible with the intracellular environment (K_d ≈ 15 nM) and yields a large change in fluorescence intensity upon binding Zn^{2+}. Replacing the fluorophore of FluoZin-3 with rhodamine resulted in the RhodZin-3 sensor, which concentrates in mitochondria due to the mitochondrial membrane potential [75].

All the sensors discussed thus far are intensity based sensors and hence exhibit limited utility for experiments requiring quantification of Zn^{2+} because the fluorescence intensity could also be affected by the sensor concentration, sample thickness, excitation source and other factors. However, a recent study developed a clever Zn^{2+} quantification method using the intensity based sensor ZPP1[76]. ZPP1 was designed based on ZP1 by replacing one pyridine arm of DPA with pyrazine. When the [ZPP1]: [Zn^{2+}] ratio is lower than 1:2, ZPP1-Zn_2 forms and emits higher fluorescence with increasing of

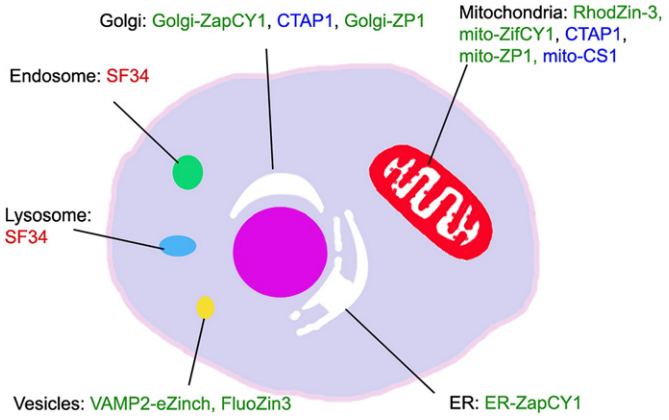

Fig. 2. Subcellular localization of metal sensors for detecting labile zinc (green), copper (blue) and iron (red) in live cells. Zinc sensor RhodZin-3 [75], mito-ZifCY1 [48], mito-ZP1 [56] and copper sensor mito-CS1 [83] are localized to mitochondria. Zinc sensor ER-ZapCY1 [51] is localized to ER. Zinc sensors VAMP2-eZinch [49] can target to vesicles. Zinc sensor FluoZin3 can report high Zn^{2+} in vesicles at rest, but its localization includes cytosol, nuclear and other unknown intracellular compartments. Iron sensor SF34 [89] is localized to lysosome and endosome. Zinc sensor Golgi-ZapCY1 [51] and Golgi-ZP1 [56] are localized to Golgi. Staining of copper sensor CTAP1 [80] showed localization of mitochondria and Golgi.

amounts of ZPP1; the intensity peaks when [ZPP1]: [Zn^{2+}] equals 1:2. When [ZPP1]: [Zn^{2+}] is higher than 1:2, the major species in solution is ZPP1-Zn_1 which displays weaker fluorescence. Using this ZPP1 titration method, the Zn^{2+} concentration can be deduced from the known ZPP1 concentrations at peak intensity [76]. This method has been used to quantify the Zn^{2+} release from Min6 cells pancreatic beta-cells [76] as well as Zn^{2+} concentrations in prostate cell lysates and mouse prostate extracts [77].

Another clever platform for generating a ratiometric indicator was employed in the development of CZ1 and CZ2 [78,79]. These are novel variants from the ZP family of zinc (II) sensors and consist of an intensity-based zinc-sensor covalently fused to coumarin via an amido-ester linker. Upon cleavage by intracellular esterases, coumarin is stoichiometrically released with the zinc-sensor, permitting ratiometric zinc-sensing relative to coumarin fluorescence.

The second design platform relies on a shift of excitation or emission profile after Zn^{2+} binding to generate ratiometric Zn^{2+} sensors. Ratiometric sensors are preferred for experiments involving quantification of Zn^{2+} concentrations because it is the change in ratio between two wavelengths, which is independent of sensor concentration, that corresponds to a specific Zn^{2+} concentration. Much effort has been put into developing small molecule ratiometric Zn^{2+} sensors based on different mechanisms which can be found from a thorough review [65]. However, none of these small molecule ratiometric sensors were used to quantify intracellular Zn^{2+} concentrations or study biological functions. Recently, genetically encoded multi-FP FRET sensors were developed in our group (ZifCY [48] family and ZapCY [51] family) and the Merkx group (eCALWY and eZinCh family [49]). In both of these sensor platforms, Zn^{2+} binding induces distance and orientation changes between donor and acceptor fluorescent proteins, resulting in a FRET change. By molecular engineering techniques, these sensors were targeted to specific subcellular regions, including the cytosol [49,51], secretory vesicles [49], endoplasmic reticulum [51] and Golgi apparatus [51], thereby permitting the quantification of their free Zn^{2+} concentrations.

4.2. Fluorescent probes for Cu^{+} /Cu^{2+}

Development and application of Cu^{+} /Cu^{2+} small molecule sensors have been hampered by the fluorescence quenching effects of Cu^{+} /Cu^{2+}. However, significant progress has been made in recent years in the development of biologically useful copper sensors showing turn-on fluorescence. For detecting Cu^{+}, the copper-responsive triarylpyrazoline (CTAP) sensor from the Fahrni group [80] and Coppersensor (CS) family from the Chang group [44,81,82] were generated. CTAP1, which is excited by UV light, gives rise to a 4.6 fold increase in fluorescence intensity in response to Cu^{+} [80]. Staining mouse fibroblast cells (NIH 3 T3) with CTAP1, as well as imaging

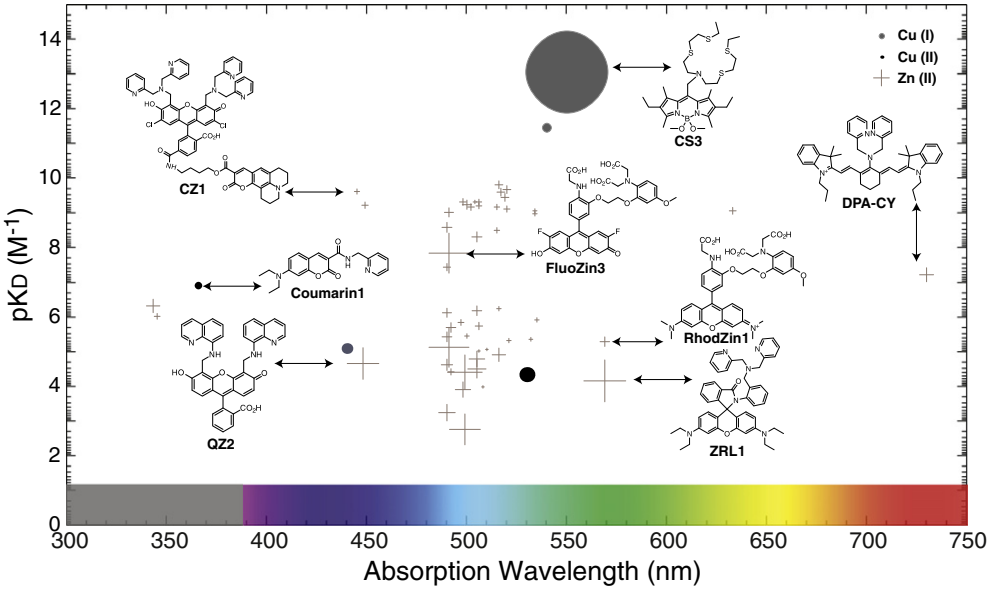

Fig. 3. Summary of major intensity-based small molecule sensors for Zn^{2+} (cross), Cu^{1+} (grey circle), and Cu^{2+} (black circle). The figure is intended to present dissociation constant (pK_D, y-axis), and absorption wavelength (x-axis). In addition, the size of a given symbol represents the relative dynamic range (defined as the change in fluorescence divided by initial fluorescence, ΔF/F, e.g., larger circles exhibit higher magnitude dynamic ranges). Featured structures include the commonly used Zn^{2+} sensors FluoZin3 and RhodZin1, a rhodamine-based lactam (ZRL1), an esterase activated sensor (CZ1) that can be ratioed to coumarin background, a cyanine (DPA-CY) based probe, and a probe with tuned affinity (QZ2) for Zn^{2+}. Also highlighted are a Cu^{2+} probe, coumarin (Coumarin1), and the highest dynamic range Cu^{1+} sensor, BODIPY (CS3). A comprehensive Table of data used to compile this Figure and associated references is presented in Supporting Information.

Table 1
Photophysical and thermodynamic properties of Zinc (II) and Copper (I) probes. The column, G.E., specifies whether the sensor is genetically encodable (Y = yes, N = no). The column DR refers to the dynamic range defined as R_{max}/R_{min}. ΔR represents the absolute change in the ratio between the bound and unbound states ($R_{max}-R_{min}$), and an asterisk (*) represents a value reported *in vivo*. Dynamic ranges determined *in vitro* often disagree with, and are typically substantially better than, dynamic ranges determined *in vivo*. Unreported or ambiguous values from the literature remain empty.

Sensor	Ligand	G.E.	λabs		λem		K_D	DR	ΔR	Ref.
			Free	Bound	Free	Bound				
CZ1	Zn(II)	N	445/505	445/505	488/534	488/534	2.50×10^{-10}	8.0	3.5	[78,79]
CZ2	Zn(II)	N	448/521	448/521	490/535	490/535		1.7*	0.4*	[78]
Fura-Zin	Zn(II)	N	378	330	510	510	2.10×10^{-6}	9.0	1.5	[41,125]
Indo-Zin	Zn(II)	N	350	350	480	395	3.00×10^{-6}			[41]
ZnAF-R2	Zn(II)	N	365	335	495	495	2.80×10^{-9}	7.0	3.1	[126]
DIPCY	Zn(II)	N	627	671	758	765	2.30×10^{-8}	1.5	0.7	[127]
ZNP1	Zn(II)	N	503/539	547	528/604	545/624	5.50×10^{-10}	17.8	6.7	[128]
DPA-COUM-4	Zn(II)	N	400	431	484	505	5.00×10^{-7}			[129]
Zinbo-5	Zn(II)	N	337	376	407	443	2.20×10^{-9}	33	33	[130]
RF3	Zn(II)	N	514	495	540	523	2.20×10^{-5}	2.4	0.8	[131]
ZTRS	Zn(II)	N	360	360	483	514	5.70×10^{-9}	30	5.8	[132]
ZapCY1	Zn(II)	Y	433/516	433/516	475/529	475/529	2.50×10^{-12}	4.1*	9.0*	[51]
ZapCY2	Zn(II)	Y	433/516	433/516	475/529	475/529	8.11×10^{-10}	1.5*	1.3*	[51]
ZifCY1	Zn(II)	Y	433/516	433/516	475/529	475/529	1.00×10^{-6}	1.4*	0.55*	[48]
ZifCY2	Zn(II)	Y	433/516	433/516	475/529	475/529	1.00×10^{-4}	2.2		[48]
ZnCh-9	Zn(II)	Y	433/516	433/516	475/529	475/539	4.43×10^{-5}	3.6	8.5	[133]
eCALWY-1	Zn(II)	Y	433/516	433/516	475/529	475/529	2.00×10^{-12}	2.0	2.0	[49]
eCALWY-2	Zn(II)	Y	433/516	433/516	475/529	475/529	9.00×10^{-12}	2.0	2.0	[49]
eCALWY-3	Zn(II)	Y	433/516	433/516	475/529	475/529	4.50×10^{-11}	1.67	1.8	[49]
eCALWY-4	Zn(II)	Y	433/516	433/516	475/529	475/529	6.30×10^{-10}	2.0	2.3	[49]
eCALWY-5	Zn(II)	Y	433/516	433/516	475/529	475/529	1.85×10^{-9}	1.8	2.5	[49]
eCALWY-6	Zn(II)	Y	433/516	433/516	475/529	475/529	2.90×10^{-9}	1.8	2.7	[49]
EZinCh	Zn(II)	Y	433/516	433/516	475/529	475/529	8.00×10^{-6}	4		[49]
RCS1	Cu(I)	N	550	548	570	556	4.00×10^{-11}	20	18	[85]
Amt1-FRET	Cu(I)	Y	433/516	433/516	475/529	475/529	2.50×10^{-18}	1.2	0.31	[50]

with synchrotron-based X-ray fluorescence microscopy showed that Cu^+ was localized in the mitochondria and Golgi [80]. CS1 is excited at visible wavelengths (λ_{ex} = 540 nm; λ_{em} = 566 nm), shows a 10-fold increase in signal when bound with Cu^+, and was used to examine copper uptake into HEK293 cells [81]. An improved sensor (CS3) with significantly improved dynamic range (75-fold change in fluorescence intensity) was successfully used in visualizing the redistribution of Cu^+ upon depolarization of hippocampal neurons [44]. CS sensors have also been engineered to target intracellular compartments, namely mitochondria. Phosphonium cations are known to accumulate in mitochondria due to the proton-gradient, and a triphenyl phosphonium moiety was incorporated into CS1 leading to accumulation of mito-CS1 in the mitochondria matrix due to the negative potential across the mitochondrial membrane [83]. Imaging experiments with Mito-CS1 indicated that this probe can monitor changes of free Cu^+ in mitochondria of HEK293T cells and human fibroblasts [83].

Given the reducing environment of the cell and the likelihood that free or accessible copper will be in the reduced form, there has been less effort in developing sensors for Cu^{2+} [65]. Recently, a coumarin-based sensor imino-coumarin (IC) for Cu^{2+} based on fluorescence enhancement by an orbital control (FEOC) mechanism was developed [84]. IC was not only applied in cultured cells, but also used in monitoring Cu^{2+} uptake in the organs of mouse [84].

The sensor platforms highlighted above are intensiometric. In an effort to develop a ratiometric Cu^{1+} sensor, a genetically encoded Cu^+ FRET sensor was reported based on the copper responsive transcriptional regulator Amt1. Amt1-FRET showed a high affinity for Cu^+ and was used to visualize Cu^+ uptake in CHO-K1 cells [50]. However, no subcellular targeting or studies using the sensor to quantify Cu^+ have been reported. Recently the Chang group developed a ratiometric version of CS1 (dubbed RCS1) by manipulating an asymmetric BODIPY platform [85]. RCS1 exhibited a 20-fold ratio change and successfully reported changes in endogenous Cu^{1+} pools in K562 erythroleukemia cells and C6 rat glioma cells [85].

4.3. Fluorescent probes for Fe^{2+}/ Fe^{3+}

Due to the quenching nature of paramagnetic Fe^{2+}/ Fe^{3+}, turn-on fluorescent sensors are rare, and none have been utilized for live cell imaging of iron in cells [65]. However, several "turn-off" probes in which Fe binding causes a decrease in fluorescence intensity have been used to study iron homeostasis in cells. Calcein is the most commonly used probe for studying Fe^{2+} homeostasis in biological systems [86–88], although it can also show nonspecific response to Fe^{3+}, Cu^{2+}, Ni^{2+} and Co^{2+}. Iron chelators such as siderophores have been utilized to develop Fe^{3+} sensors and interested readers can find a few examples in a previous comprehensive review [65]. A new Fe^{3+} sensor SF34 based on a 3-hydroxypyridin-4-one (HPO) chelation unit was found to be sequestered into vesicles in murine bone marrow derived macrophages. Imaging experiments by confocal microscopy showed that the probe is localized to endosomes and/or lysosomes and responds to fluctuations in extracellular iron [89].

4.4. Fluorescent probes for Mg^{2+}

An excellent recent review highlights the current status and recent advances in fluorescent indicators for Mg^{2+} [90]. In brief, several ratiometric and intensity-based Mg^{2+} small molecule sensors have been developed based on the binding platform APTRA (o-aminophenol-N,N,O-triacetic acid). However, the metal specificity of these indicators is generally not satisfactory because these sensors also bind cations such as Ca^{2+} and Zn^{2+}. Mag-fura-2 (Invitrogen) is the most widely used indicator for quantification of biological Mg^{2+}, although newer and more specific Mg^{2+} sensors have been developed recently [90].

4.5. Fluorescent probes for Ni^{2+}

There are very few reports of Ni^{2+}-specific indicators for live cell imaging. The Chang group recently reported a specific Ni^{2+} sensor

Nickelsensor-1 (NS1) by attaching a BODIPY fluorophore to a mixed N/O/S receptor [91]. This probe displays a 25-fold increase in fluorescence and binds Ni^{2+} with low affinity ($K_d = 193\ \mu M$). Staining of human lung carcinoma A549 cells showed that the intracellular Ni^{2+} concentration increased upon incubation of extracellular $NiCl_2$ (1 mM). This sensor provides a prototype to engineer more promising Ni^{2+} sensor with a higher dynamic range and altered affinity.

4.6. Fluorescent probes for toxic metals

Although Cd^{2+} is not an endogenous metal ion in mammalian cells, there is significant interest in the development of fluorescent indicators to examine Cd^{2+} toxicity. A compound composed of fluorescein and thiosemicarbazide showed selective response to Cd^{2+} with 2.5 fold of dynamic ratio and also was used in HK-2 cells [92]. A BODIPY sensor with high dynamic ratio (195 fold) was generated and imaged in HeLa cells [93]. Another compound based on 8-Hydroxyquinoline was also tested in cultured cells for imaging, but with low dynamic range [94]. The near-infrared fluorescent sensor CYP family was generated based on tricabocyanine [95]. Several ratiometric sensors were also synthesized and used for imaging in cells. One sensor was designed based on an internal charge transfer (ICT) mechanism and applied for imaging in PC12 cells [96]. Another ratiometric sensor DBITA showed high selectivity and sensitivity (picomolar) to Cd^{2+}. A new sensor DQCd1 was generated based on the fluorophore 4-isobutoxy-6-(dimethylamino)-8-ethoxyquinaldine showed high dynamic ratio (15 fold) and high affinity ($K_d = 41$pM) to Cd^{2+} [97]. In addition, the first genetically encoded Cd^{2+} sensor was generated by modifying a Zn^{2+} FRET sensor. By introducing four cysteine residues on the FRET pair fluorescent proteins, the sensor Cd-FRET showed high selectivity for Cd^{2+} over Zn^{2+} [52].

Lead (Pb^{2+}) pollution is a serious hazard to the environment and human health, and poses a particular risk for development of the nervous system in children [98]. Fluorescent sensors for Pb^{2+} have been developed based on different hybrid platforms including fluorophore and peptide [99], protein and DNA duplex [100], DNAzyme and nanoparticles [101,102]. Among these, a platform utilizing dsDNA binding to protein developed by the He lab is particularly novel. In this platform, a fluorescent DNA base analogue, pyrrolo-C, was inserted into the middle of the PbrR-binding sequence. When the pyrrolo-C pairs with G its fluorescence is quenched. Binding of Pb^{2+} to the PbrR protein causes DNA distortion, resulting in recovery of the fluorescence of pyrrolo-C. However, none of the sensors based on this platform have been used in living cells. In addition, a few small molecule sensors for Pb^{2+} have been explored [103–105], but only one Leadfluor-1 (LF1) was applied in living mammalian cells for imaging [104].

Mercury is another toxic metal of substantial interest. Fluorescent tools to detect free Hg^{2+} have been developed mostly based on rhodamine and these sensors have been applied in living cells [106–109]. For example, recently a rhodamine based chemosensor RS1, which combined a furaldehyde and a thiospirolactam rhodamine chromophore was used in rat Schwann cells [109]. Lastly, a protein-DNA duplex hybrid platform, similar to the sensor for Pb2+ described above has been used to create a highly selective ratiometric Hg^{2+} sensor based on the transcription factor MerR [110].

5. Outlook

Over the past decade, there have been remarkable advances in our ability to image metal ions in living cells with high spatial and temporal resolution using fluorescence microscopy. Still, many of these existing tools could benefit from improved signal-to-noise, increased imaging modalities such as chemi/bioluminescence. Additionally, while the available probes for Zn^{2+} and Cu^{1+} have enabled exciting discoveries about the dynamic nature of metal ion pools [44,51,111], there is a significant need to expand the toolbox to include biologically important ions such as $Mn^{2+/3+}$, Mg^{2+}, $Fe^{2+/3+}$, Ni^{2+}, and others. But, addressing questions such as “where are labile metals located; how are metal “signals” modulated; and what are the consequences of metal mobilization?” is likely to require more than just probes and analytical techniques for visualizing metal ions. For example, the field would benefit immensely from an expanded toolbox for probing, perturbing, and controlling metal ion fluxes in cells. Two such tools are versatile and specific metal chelators and photoactive caged metal compounds.

Specific metal chelators offer the opportunity to reduce or limit metal ion availability and are crucial tools for determining the function of metal ion fluxes. For example, the development of 1,2-bis(*o*-aminophenoxy)ethane-N,N,N′,N′-tetraacetic acid (BAPTA) [37] was instrumental in elucidating the nature and function of different Ca^{2+} signals. BAPTA exhibits high selectivity for Ca^{2+} over Mg^{2+}, lower pKas for the nitrogen ligands, and faster binding and release kinetics than traditional chelators such as ethylene glycol bis(β-aminoethyl ether)-N,N,N′,N′-tetraacetic acid (EGTA). These characteristics have made BAPTA an invaluable tool for dissecting Ca^{2+} signals, where the slow kinetics of EGTA make it an ideal tool for preventing global Ca^{2+} signals, revealing local release events, and the fast kinetics of BAPTA make it ideal for abolishing local Ca^{2+} signals [112,113]. Given the likely heterogeneous distribution of metal ions at the subcellular level, chelators with differential membrane permeability should enable differentiation of intra- versus extra-cellular signaling. Recently the Lippard lab generated a new membrane-impermeable Zn^{2+} chelator, ZX1, that permitted rapid and selective chelation of extracellular Zn^{2+} released from mossy fiber neurons, revealing a new mechanism for modulation of synaptic strength [114]. The studies highlighted above reveal that chelators with differential selectivity, kinetics, and membrane permeability can help dissect the nature and function of metal signals. More tools of this nature would be an invaluable resource for elucidating the properties and consequences of metal ion signals.

In a general sense, “caged compounds” represent bioreagents that are released or become active upon exposure to light. A handful of excellent reviews detail the design and application of such reagents for illuminating cell biology [115–117]. Molecular design of caged compounds involves the use of photo-labile chelating cages, such that exposure to UV-light results in degradation of the cage, releasing the ion or molecule. Such tools permit precise spatial and temporal control of the caged molecule or ion in cells and were instrumental in revealing how oscillatory Ca^{2+} signals are decoded by cells [118]. Although there are no caged metal complexes that been used in live cells, advances have been made in recent years for the development and characterization of caged-Zn^{2+}, ZinCleave-1 and 2, [119,120], and one Cu^{2+} [121,122]. In an alternative approach, the genetically encodeable light oxygen voltage (LOV) domain has been used as a light-induced protein switch, giving rise to local activation of GTPases [123] and control of Ca^{2+} signals [124], although this approach has not yet been applied to other metal ions. These tools have the potential to transform our understanding of metal dynamics in cells by offering the promise of precisely controlling metal ion availability in specific locations and at specific times in cells.

Acknowledgements

We would like to thank J. Genevieve Park for careful reading of this manuscript. The authors would like to thank the NIH (GM084027 to A.E.P.) for financial support. K.M.D. was supported by an NIH Biophysics Training Grant (T32 GM-065103) and NSF IGERT on Computational Optical Sensing Imaging (0801680).

Appendix A. Supplementary materials

Supplementary data to this article can be found online at http://dx.doi.org/10.1016/j.bbamcr.2012.04.001.

References

[1] W.I. Vonk, L.W. Klomp, Role of transition metals in the pathogenesis of amyotrophic lateral sclerosis, Biochem. Soc. Trans. 36 (2008) 1322–1328.
[2] J. Jansen, W. Karges, L. Rink, Zinc and diabetes—clinical links and molecular mechanisms, J. Nutr. Biochem. 20 (2009) 399–417.
[3] L.A. Lichten, R.J. Cousins, Mammalian zinc transporters: nutritional and physiologic regulation, Annu. Rev. Nutr. 29 (2009) 153–176.
[4] M.L. Turski, D.J. Thiele, New roles for copper metabolism in cell proliferation, signaling, and disease, J. Biol. Chem. 284 (2009) 717–721.
[5] T. Ganz, E. Nemeth, Hepcidin and disorders of iron metabolism, Annu. Rev. Med. 62 (2011) 347–360.
[6] R.D. Bloomberg, A. Fleishman, J.E. Nalle, D.M. Herron, S. Kini, Nutritional deficiencies following bariatric surgery: what have we learned? Obes. Surg. 15 (2005) 145–154.
[7] R.E. Fleming, P. Ponka, Iron overload in human disease, N. Engl. J. Med. 366 (2012) 348–359.
[8] A.S. Prasad, Zinc deficiency in patients with sickle cell disease, Am. J. Clin. Nutr. 75 (2002) 181–182.
[9] Y.J. Kang, Z. Zhou, Zinc prevention and treatment of alcoholic liver disease, Mol. Aspects Med. 26 (2005) 391–404.
[10] I. Bertini, H.B. Gray, E.I. Stiefel, J.S. Valentine, Biological Inorganic Chemistry, University Science Books, Sausalito, 2007.
[11] C.J. Fahrni, Biological applications of X-ray fluorescence microscopy: exploring the subcellular topography and speciation of transition metals, Curr. Opin. Chem. Biol. 11 (2007) 121–127.
[12] D.W. Domaille, E.L. Que, C.J. Chang, Synthetic fluorescent sensors for studying the cell biology of metals, Nat. Chem. Biol. 4 (2008) 168–175.
[13] S. Tottey, K.J. Waldron, S.J. Firbank, B. Reale, C. Bessant, K. Sato, T.R. Cheek, J. Gray, M.J. Banfield, C. Dennison, N.J. Robinson, Protein-folding location can regulate manganese-binding versus copper- or zinc-binding, Nature 455 (2008) 1138–1142.
[14] A.W. Foster, N.J. Robinson, Promiscuity and preferences of metallothioneins: the cell rules, BMC Biol. 9 (2011) 25.
[15] D.J. Eide, Zinc transporters and the cellular trafficking of zinc, Biochim. Biophys. Acta 1763 (2006) 711–722.
[16] B.E. Kim, T. Nevitt, D.J. Thiele, Mechanisms for copper acquisition, distribution and regulation, Nat. Chem. Biol. 4 (2008) 176–185.
[17] I. De Domenico, D. McVey Ward, J. Kaplan, Regulation of iron acquisition and storage: consequences for iron-linked disorders, Nat. Rev. Mol. Cell Biol. 9 (2008) 72–81.
[18] S. Yamasaki, K. Sakata-Sogawa, A. Hasegawa, T. Suzuki, K. Kabu, E. Sato, T. Kurosaki, S. Yamashita, M. Tokunaga, K. Nishida, T. Hirano, Zinc is a novel intracellular second messenger, J. Cell Biol. 177 (2007) 637–645.
[19] Z. Qin, J.A. Caruso, B. Lai, A. Matusch, J.S. Becker, Trace metal imaging with high spatial resolution: applications in biomedicine, Metallomics 3 (2011) 28–37.
[20] N. Kapp, D. Studer, P. Gehr, M. Geiser, Electron energy-loss spectroscopy as a tool for elemental analysis in biological specimens, Methods Mol. Biol. 369 (2007) 431–447.
[21] M. Morello, A. Canini, P. Mattioli, R.P. Sorge, A. Alimonti, B. Bocca, G. Forte, A. Martorana, G. Bernardi, G. Sancesario, Sub-cellular localization of manganese in the basal ganglia of normal and manganese-treated rats An electron spectroscopy imaging and electron energy-loss spectroscopy study, Neurotoxicology 29 (2008) 60–72.
[22] M. Ralle, S. Lutsenko, Quantitative imaging of metals in tissues, Biometals 22 (2009) 197–205.
[23] R. Yuste, Fluorescence microscopy today, Nat. Methods 2 (2005) 902–904.
[24] J.W. Lichtman, J.A. Conchello, Fluorescence microscopy, Nat. Methods 2 (2005) 910–919.
[25] P. Timpson, E.J. McGhee, K.I. Anderson, Imaging molecular dynamics in vivo–from cell biology to animal models, J. Cell Sci. 124 (2011) 2877–2890.
[26] M.J. Pittet, R. Weissleder, Intravital imaging, Cell 147 (2011) 983–991.
[27] Y. You, S. Lee, T. Kim, K. Ohkubo, W.S. Chae, S. Fukuzumi, G.J. Jhon, W. Nam, S.J. Lippard, Phosphorescent sensor for biological mobile zinc, J. Am. Chem. Soc. 133 (2011) 18328–18342.
[28] T.C. Doyle, S.M. Burns, C.H. Contag, In vivo bioluminescence imaging for integrated studies of infection, Cell. Microbiol. 6 (2004) 303–317.
[29] N. Andreu, A. Zelmer, S. Wiles, Noninvasive biophotonic imaging for studies of infectious disease, FEMS Microbiol. Rev. 35 (2011) 360–394.
[30] G.D. Luker, J.P. Bardill, J.L. Prior, C.M. Pica, D. Piwnica-Worms, D.A. Leib, Noninvasive bioluminescence imaging of herpes simplex virus type 1 infection and therapy in living mice, J. Virol. 76 (2002) 12149–12161.
[31] L.I. Jiang, J. Collins, R. Davis, K.M. Lin, D. DeCamp, T. Roach, R. Hsueh, R.A. Rebres, E.M. Ross, R. Taussig, I. Fraser, P.C. Sternweis, Use of a cAMP BRET sensor to characterize a novel regulation of cAMP by the sphingosine 1-phosphate/G13 pathway, J. Biol. Chem. 282 (2007) 10576–10584.
[32] L. Zhang, K.C. Lee, M.S. Bhojani, A.P. Khan, A. Shilman, E.C. Holland, B.D. Ross, A. Rehemtulla, Molecular imaging of Akt kinase activity, Nat. Med. 13 (2007) 1114–1119.
[33] K.J. Herbst, M.D. Allen, J. Zhang, Luminescent kinase activity biosensors based on a versatile bimolecular switch, J. Am. Chem. Soc. 133 (2011) 5676–5679.
[34] E.L. Que, C.J. Chang, Responsive magnetic resonance imaging contrast agents as chemical sensors for metals in biology and medicine, Chem. Soc. Rev. 39 (2010) 51–60.
[35] C.S. Bonnet, E. Toth, MRI probes for sensing biologically relevant metal ions, Future Med. Chem. 2 (2010) 367–384.
[36] A. Keppler, S. Gendreizig, T. Gronemeyer, H. Pick, H. Vogel, K. Johnsson, A general method for the covalent labeling of fusion proteins with small molecules in vivo, Nat. Biotechnol. 21 (2003) 86–89.
[37] R.Y. Tsien, New calcium indicators and buffers with high selectivity against magnesium and protons: design, synthesis, and properties of prototype structures, Biochemistry 19 (1980) 2396–2404.
[38] G. Grynkiewicz, M. Poenie, R.Y. Tsien, A New Generation of Ca^{2+} Indicators with Greatly Improved Fluorescence Properties, J. Biol. Chem. 260 (1985) 3440–3450.
[39] R.Y. Tsien, Fluorescent Indicators of ion concentrations, Methods Cell Biol. 30 (1989) 127–156.
[40] J.R. Lakowicz, Principles of Fluorescence Spectroscopy, 2nd ed. Kluwer Academic Press, New York, 1999.
[41] K.R. Gee, Z.L. Zhou, D. Ton-That, S.L. Sensi, J.H. Weiss, Measuring zinc in living cells. A new generation of sensitive and selective fluorescent probes, Cell Calcium 31 (2002) 245–251.
[42] P. Du, S.J. Lippard, A highly selective turn-on colorimetric, red fluorescent sensor for detecting mobile zinc in living cells, Inorg. Chem. 49 (2010) 10753–10755.
[43] K. Komatsu, K. Kikuchi, H. Kojima, Y. Urano, T. Nagano, Selective zinc sensor molecules with various affinities for Zn2+, revealing dynamics and regional distribution of synaptically released Zn2+ in hippocampal slices, J. Am. Chem. Soc. 127 (2005) 10197–10204.
[44] S.C. Dodani, D.W. Domaille, C.I. Nam, E.W. Miller, L.A. Finney, S. Vogt, C.J. Chang, Calcium-dependent copper redistributions in neuronal cells revealed by a fluorescent copper sensor and X-ray fluorescence microscopy, Proc. Natl. Acad. Sci. U. S. A. 108 (2011) 5980–5985.
[45] R.Y. Tsien, A non-disruptive technique for loading calcium buffers and indicators into cells, Nature 290 (1981) 527–528.
[46] L. Tian, S.A. Hires, T. Mao, D. Huber, M.E. Chiappe, S.H. Chalasani, L. Petreanu, J. Akerboom, S.A. McKinney, E.R. Schreiter, C.I. Bargmann, V. Jayaraman, K. Svoboda, L.L. Looger, Imaging neural activity in worms, flies and mice with improved GCaMP calcium indicators, Nat. Methods 6 (2009) 875–881.
[47] Y. Zhao, S. Araki, J. Wu, T. Teramoto, Y.F. Chang, M. Nakano, A.S. Abdelfattah, M. Fujiwara, T. Ishihara, T. Nagai, R.E. Campbell, An expanded palette of genetically encoded Ca(2+) indicators, Science 333 (2011) 1888–1891.
[48] P.J. Dittmer, J.G. Miranda, J.A. Gorski, A.E. Palmer, Genetically encoded sensors to elucidate spatial distribution of cellular zinc, J. Biol. Chem. 284 (2009) 16289–16297.
[49] J.L. Vinkenborg, T.J. Nicolson, E.A. Bellomo, M.S. Koay, G.A. Rutter, M. Merkx, Genetically encoded FRET sensors to monitor intracellular Zn2+ homeostasis, Nat. Methods 6 (2009) 737–740.
[50] S.V. Wegner, H. Arslan, M. Sunbul, J. Yin, C. He, Dynamic copper(I) imaging in mammalian cells with a genetically encoded fluorescent copper(I) sensor, J. Am. Chem. Soc. 132 (2010) 2567–2569.
[51] Y. Qin, P.J. Dittmer, J.G. Park, K.B. Jansen, A.E. Palmer, Measuring steady-state and dynamic endoplasmic reticulum and Golgi Zn2+ with genetically encoded sensors, Proc. Natl. Acad. Sci. U. S. A. 108 (2011) 7351–7356.
[52] J.L. Vinkenborg, S.M. van Duijnhoven, M. Merkx, Reengineering of a fluorescent zinc sensor protein yields the first genetically encoded cadmium probe, Chem. Commun. (Camb.) 47 (2011) 11879–11881.
[53] S.B. VanEngelenburg, A.E. Palmer, Fluorescent biosensors of protein function, Curr. Opin. Chem. Biol. 12 (2008) 60–65.
[54] R.H. Newman, M.D. Fosbrink, J. Zhang, Genetically encodable fluorescent biosensors for tracking signaling dynamics in living cells, Chem. Rev. 111 (2011) 3614–3666.
[55] D.J. Wallace, S. Meyer zum Alten Borgloh, S. Astori, Y. Yang, M. Bausen, S. Kugler, A.E. Palmer, R.Y. Tsien, R. Sprengel, J.N. Kerr, W. Denk, M.T. Hasan, Single-spike detection in vitro and in vivo with a genetic Ca2+ sensor, Nat. Methods 5 (2008) 797–804.
[56] E. Tomat, E.M. Nolan, J. Jaworski, S.J. Lippard, Organelle-specific zinc detection using zinpyr-labeled fusion proteins in live cells, J. Am. Chem. Soc. 130 (2008) 15776–15777.
[57] M. Bannwarth, J.I.R. Correa, M. Sztretye, S. Pouvreau, C. Fellay, A. Aebischer, L. Royer, E. Rios, K. Johnsson, Indo-1 Derivatives for Local Calcium Sensing, ACS Chem. Biol. 4 (2009) 179–190.
[58] M. Kamiya, K. Johnsson, Localizable and highly sensitive calcium indicator based on a BODIPY fluorophore, Anal. Chem. 82 (2010) 6472–6479.
[59] O. Tour, S.R. Adams, R.A. Kerr, R.M. Meijer, T.J. Sejnowski, R.W. Tsien, R.Y. Tsien, Calcium Green FlAsH as a genetically targeted small-molecule calcium indicator, Nat. Chem. Biol. 3 (2007) 423–431.
[60] K.M. Marks, M. Rosinov, G.P. Nolan, In Vivo Targeting of Organic Calcium Sensors via Genetically Selected Peptides, Chem. Biol. 11 (2004) 347–356.
[61] A. Krezel, W. Maret, Zinc-buffering capacity of a eukaryotic cell at physiological pZn, J. Biol. Inorg. Chem. 11 (2006) 1049–1062.
[62] H.J., D. Mahanand, Fluorometric determination of zinc in biologic fluids, Clin. Chem. 14 (1968) 6–11.
[63] C.J. Frederickson, E.J. Kasarskis, D. Ringo, R.E. Frederickson, A quinoline fluorescence method for visualizing and assaying the histochemically reactive zinc (bouton zinc) in the brain, J. Neurosci. Methods 20 (1987) 91–103.
[64] P.D. Zalewski, I.J. Forbes, W.H. Betts, Correlation of apoptosis with change in intracellular labile Zn(II) using zinquin [(2-methyl-8-p-toluenesulphonamido-6-quinolyloxy)acetic acid], a new specific fluorescent probe for Zn(II), Biochem. J. 296 (Pt 2) (1993) 403–408.
[65] E.L. Que, D.W. Domaille, C.J. Chang, Metals in neurobiology: probing their chemistry and biology with molecular imaging, Chem. Rev. 108 (2008) 1517–1549.
[66] M.D. Pluth, E. Tomat, S.J. Lippard, Biochemistry of mobile zinc and nitric oxide revealed by fluorescent sensors, Annu. Rev. Biochem. 80 (2011) 333–355.

[67] S.C. Burdette, G.K. Walkup, B. Spingler, R.Y. Tsien, S.J. Lippard, Fluorescent sensors for Zn(2+) based on a fluorescein platform: synthesis, properties and intracellular distribution, J. Am. Chem. Soc. 123 (2001) 7831–7841.
[68] C.J. Chang, E.M. Nolan, J. Jaworski, S.C. Burdette, M. Sheng, S.J. Lippard, Bright fluorescent chemosensor platforms for imaging endogenous pools of neuronal zinc, Chem. Biol. 11 (2004) 203–210.
[69] S.C. Burdette, C.J. Frederickson, W. Bu, S.J. Lippard, ZP4, an improved neuronal Zn2+ sensor of the Zinpyr family, J. Am. Chem. Soc. 125 (2003) 1778–1787.
[70] E.M. Nolan, S.J. Lippard, The zinspy family of fluorescent zinc sensors: syntheses and spectroscopic investigations, Inorg. Chem. 43 (2004) 8310–8317.
[71] E.M. Nolan, J.W. Ryu, J. Jaworski, R.P. Feazell, M. Sheng, S.J. Lippard, Zinspy sensors with enhanced dynamic range for imaging neuronal cell zinc uptake and mobilization, J. Am. Chem. Soc. 128 (2006) 15517–15528.
[72] T. Hirano, K. Kikuchi, Y. Urano, T. Nagano, Improvement and biological applications of fluorescent probes for zinc, ZnAFs, J. Am. Chem. Soc. 124 (2002) 6555–6562.
[73] E.M. Nolan, J. Jaworski, K. Okamoto, Y. Hayashi, M. Sheng, S.J. Lippard, QZ1 and QZ2: rapid, reversible quinoline-derivatized fluoresceins for sensing biological Zn(II), J. Am. Chem. Soc. 127 (2005) 16812–16823.
[74] Y. Wu, X. Peng, B. Guo, J. Fan, Z. Zhang, J. Wang, A. Cui, Y. Gao, Boron dipyrromethene fluorophore based fluorescence sensor for the selective imaging of Zn(II) in living cells, Org. Biomol. Chem. 3 (2005) 1387–1392.
[75] S.L. Sensi, D. Ton-That, J.H. Weiss, A. Rothe, K.R. Gee, A new mitochondrial fluorescent zinc sensor, Cell Calcium 34 (2003) 281–284.
[76] X.A. Zhang, D. Hayes, S.J. Smith, S. Friedle, S.J. Lippard, New strategy for quantifying biological zinc by a modified zinpyr fluorescence sensor, J. Am. Chem. Soc. 130 (2008) 15788–15789.
[77] S.K. Ghosh, P. Kim, X.A. Zhang, S.H. Yun, A. Moore, S.J. Lippard, Z. Medarova, A novel imaging approach for early detection of prostate cancer based on endogenous zinc sensing, Cancer Res. 70 (2010) 6119–6127.
[78] C.C. Woodroofe, A.C. Won, S.J. Lippard, Esterase-activated two-fluorophore system for ratiometric sensing of biological zinc(II), Inorg. Chem. 44 (2005) 3112–3120.
[79] C.C. Woodroofe, S.J. Lippard, A novel two-fluorophore approach to ratiometric sensing of Zn(2+), J. Am. Chem. Soc. 125 (2003) 11458–11459.
[80] L. Yang, R. McRae, M.M. Henary, R. Patel, B. Lai, S. Vogt, C.J. Fahrni, Imaging of the intracellular topography of copper with a fluorescent sensor and by synchrotron x-ray fluorescence microscopy, Proc. Natl. Acad. Sci. U. S. A. 102 (2005) 11179–11184.
[81] L. Zeng, E.W. Miller, A. Pralle, E.Y. Isacoff, C.J. Chang, A selective turn-on fluorescent sensor for imaging copper in living cells, J. Am. Chem. Soc. 128 (2006) 10–11.
[82] E.W. Miller, L. Zeng, D.W. Domaille, C.J. Chang, Preparation and use of Coppersensor-1, a synthetic fluorophore for live-cell copper imaging, Nat. Protoc. 1 (2006) 824–827.
[83] S.C. Dodani, S.C. Leary, P.A. Cobine, D.R. Winge, C.J. Chang, A targetable fluorescent sensor reveals that copper-deficient SCO1 and SCO2 patient cells prioritize mitochondrial copper homeostasis, J. Am. Chem. Soc. 133 (2011) 8606–8616.
[84] K.C. Ko, J.S. Wu, H.J. Kim, P.S. Kwon, J.W. Kim, R.A. Bartsch, J.Y. Lee, J.S. Kim, Rationally designed fluorescence 'turn-on' sensor for Cu2+, Chem. Commun. (Camb.) 47 (2011) 3165–3167.
[85] D.W. Domaille, L. Zeng, C.J. Chang, Visualizing ascorbate-triggered release of labile copper within living cells using a ratiometric fluorescent sensor, J. Am. Chem. Soc. 132 (2010) 1194–1195.
[86] D.J. Lane, S.R. Robinson, H. Czerwinska, G.M. Bishop, A. Lawen, Two routes of iron accumulation in astrocytes: ascorbate-dependent ferrous iron uptake via the divalent metal transporter (DMT1) plus an independent route for ferric iron, Biochem. J. 432 (2010) 123–132.
[87] H. Glickstein, R.B. El, G. Link, W. Breuer, A.M. Konijn, C. Hershko, H. Nick, Z.I. Cabantchik, Action of chelators in iron-loaded cardiac cells: Accessibility to intracellular labile iron and functional consequences, Blood 108 (2006) 3195–3203.
[88] M. Shvartsman, R. Kikkeri, A. Shanzer, Z.I. Cabantchik, Non-transferrin-bound iron reaches mitochondria by a chelator-inaccessible mechanism: biological and clinical implications, Am. J. Physiol. Cell Physiol. 293 (2007) C1383–C1394.
[89] S. Fakih, M. Podinovskaia, X. Kong, U.E. Schaible, H.L. Collins, R.C. Hider, Monitoring intracellular labile iron pools: A novel fluorescent iron(III) sensor as a potential non-invasive diagnosis tool, J. Pharm. Sci. 98 (2009) 2212–2226.
[90] V. Trapani, G. Farruggia, C. Marraccini, S. Iotti, A. Cittadini, F.I. Wolf, Intracellular magnesium detection: imaging a brighter future, Analyst 135 (2010) 1855–1866.
[91] S.C. Dodani, Q. He, C.J. Chang, A turn-on fluorescent sensor for detecting nickel in living cells, J. Am. Chem. Soc. 131 (2009) 18020–18021.
[92] W. Liu, L. Xu, R. Sheng, P. Wang, H. Li, S. Wu, A water-soluble "switching on" fluorescent chemosensor of selectivity to Cd2+, Org. Lett. 9 (2007) 3829–3832.
[93] T. Cheng, Y. Xu, S. Zhang, W. Zhu, X. Qian, L. Duan, A highly sensitive and selective OFF-ON fluorescent sensor for cadmium in aqueous solution and living cell, J. Am. Chem. Soc. 130 (2008) 16160–16161.
[94] M. Mameli, M.C. Aragoni, M. Arca, C. Caltagirone, F. Demartin, G. Farruggia, G. De Filippo, F.A. Devillanova, A. Garau, F. Isaia, V. Lippolis, S. Murgia, L. Prodi, A. Pintus, N. Zaccheroni, A selective, nontoxic, OFF-ON fluorescent molecular sensor based on 8-hydroxyquinoline for probing Cd(2+) in living cells, Chemistry 16 (2010) 919–930.
[95] Y. Yang, T. Cheng, W. Zhu, Y. Xu, X. Qian, Highly selective and sensitive near-infrared fluorescent sensors for cadmium in aqueous solution, Org. Lett. 13 (2011) 264–267.
[96] X. Peng, J. Du, J. Fan, J. Wang, Y. Wu, J. Zhao, S. Sun, T. Xu, A selective fluorescent sensor for imaging Cd2+ in living cells, J. Am. Chem. Soc. 129 (2007) 1500–1501.
[97] L. Xue, G. Li, Q. Liu, H. Wang, C. Liu, X. Ding, S. He, H. Jiang, Ratiometric fluorescent sensor based on inhibition of resonance for detection of cadmium in aqueous solution and living cells, Inorg. Chem. 50 (2011) 3680–3690.
[98] L. Jarup, Hazards of heavy metal contamination, Br. Med. Bull. 68 (2003) 167–182.
[99] S.G. Deo, Hilary Arnold, A Selective, Ratiometric Fluorescent Sensor for Pb2+, J. Am. Chem. Soc. 122 (2000) 2.
[100] P. Chen, B. Greenberg, S. Taghavi, C. Romano, D. van der Lelie, C. He, An exceptionally selective lead(II)-regulatory protein from Ralstonia metallidurans: development of a fluorescent lead(II) probe, Angew. Chem. Int. Ed. Engl. 44 (2005) 2715–2719.
[101] J. Liu, Y. Lu, Accelerated color change of gold nanoparticles assembled by DNAzymes for simple and fast colorimetric Pb2+ detection, J. Am. Chem. Soc. 126 (2004) 12298–12305.
[102] L. Wang, Y. Jin, J. Deng, G. Chen, Gold nanorods-based FRET assay for sensitive detection of Pb2+ using 8-17DNAzyme, Analyst 136 (2011) 5169–5174.
[103] X.L. Ni, S. Wang, X. Zeng, Z. Tao, T. Yamato, Pyrene-linked triazole-modified homooxacalix[3]arene: a unique C3 symmetry ratiometric fluorescent chemosensor for Pb2+, Org. Lett. 13 (2011) 552–555.
[104] Q. He, E.W. Miller, A.P. Wong, C.J. Chang, A selective fluorescent sensor for detecting lead in living cells, J. Am. Chem. Soc. 128 (2006) 9316–9317.
[105] C. Hou, X. Yijia, Na Fu, Caitlin C. Jacquot, Thomas C. Squier, Haishi Cao, Turn-on ratiometric fluorescent sensor for Pb2+ detection, Tetrahedron Lett. 52 (2011) 4.
[106] W. Lin, X. Cao, Y. Ding, L. Yuan, Q. Yu, A reversible fluorescent Hg2+ chemosensor based on a receptor composed of a thiol atom and an alkene moiety for living cell fluorescence imaging, Org. Biomol. Chem. 8 (2010) 3618–3620.
[107] W. Huang, P. Zhou, W. Yan, C. He, L. Xiong, F. Li, C. Duan, A bright water-compatible sugar-rhodamine fluorescence sensor for selective detection of Hg2+ in natural water and living cells, J. Environ. Monit. 11 (2009) 330–335.
[108] H. Yang, Z. Zhou, K. Huang, M. Yu, F. Li, T. Yi, C. Huang, Multisignaling optical-electrochemical sensor for Hg2+ based on a rhodamine derivative with a ferrocene unit, Org. Lett. 9 (2007) 4729–4732.
[109] H. Wang, Y. Li, S. Xu, C. Zhou, X. Fei, L. Sun, C. Zhang, Q. Yang, X. Xu, Rhodamine--based highly sensitive colorimetric off-on fluorescent chemosensor for Hg2+ in aqueous solution and for live cell imaging, Org. Biomol. Chem. 9 (2011) 2850–2855.
[110] S.V. Wegner, A. Okesli, P. Chen, C. He, Design of an emission ratiometric biosensor from MerR family proteins: a sensitive and selective sensor for Hg2+, J. Am. Chem. Soc. 129 (2007) 3474–3475.
[111] A.M. Kim, M.L. Bernhardt, B.Y. Kong, R.W. Ahn, S. Vogt, T.K. Woodruff, T.V. O'Halloran, Zinc sparks are triggered by fertilization and facilitate cell cycle resumption in mammalian eggs, ACS Chem. Biol. 6 (2011) 716–723.
[112] S.L. Dargan, I. Parker, Buffer kinetics shape the spatiotemporal patterns of IP3-evoked Ca2+ signals, J. Physiol. 553 (2003) 775–788.
[113] S.L. Dargan, B. Schwaller, I. Parker, Spatiotemporal patterning of IP3-mediated Ca2+ signals in Xenopus oocytes by Ca2+—binding proteins, J. Physiol. 556 (2004) 447–461.
[114] E. Pan, X.A. Zhang, Z. Huang, A. Krezel, M. Zhao, C.E. Tinberg, S.J. Lippard, J.O. McNamara, Vesicular zinc promotes presynaptic and inhibits postsynaptic long-term potentiation of mossy fiber-CA3 synapse, Neuron 71 (2011) 1116–1126.
[115] G. Mayer, A. Heckel, Biologically active molecules with a "light switch", Angew. Chem. Int. Ed. Engl. 45 (2006) 4900–4921.
[116] G.C. Ellis-Davies, Caged compounds: photorelease technology for control of cellular chemistry and physiology, Nat. Methods 4 (2007) 619–628.
[117] H.M. Lee, D.R. Larson, D.S. Lawrence, Illuminating the chemistry of life: design, synthesis, and applications of "caged" and related photoresponsive compounds, ACS Chem. Biol. 4 (2009) 409–427.
[118] W.-h. Li, J. Llopis, M. Whitney, G. Zlokarnik, R.Y. Tsien, Cell-permeant caged $InsP_3$ ester shows that Ca^{2+} spike frequency can optimize gene expression, Nature 392 (1998) 936–941.
[119] H.M. Bandara, D.P. Kennedy, E. Akin, C.D. Incarvito, S.C. Burdette, Photoinduced release of Zn2+ with ZinCleav-1: a nitrobenzyl-based caged complex, Inorg. Chem. 48 (2009) 8445–8455.
[120] H.M. Bandara, T.P. Walsh, S.C. Burdette, A Second-generation photocage for Zn2+ inspired by TPEN: characterization and insight into the uncaging quantum yields of ZinCleav chelators, Chemistry 17 (2011) 3932–3941.
[121] K.L. Ciesienski, K.L. Haas, M.G. Dickens, Y.T. Tesema, K.J. Franz, A photolabile ligand for light-activated release of caged copper, J. Am. Chem. Soc. 130 (2008) 12246–12247.
[122] K.L. Ciesienski, K.L. Haas, K.J. Franz, Development of next-generation photolabile copper cages with improved copper binding properties, Dalton Trans. 39 (2010) 9538–9546.
[123] Y.I. Wu, D. Frey, O.I. Lungu, A. Jaehrig, I. Schlichting, B. Kuhlman, K.M. Hahn, A genetically encoded photoactivatable Rac controls the motility of living cells, Nature 461 (2009) 104–108.
[124] E. Pham, E. Mills, K. Truong, A synthetic photoactivated protein to generate local or global Ca(2+) signals, Chem. Biol. 18 (2011) 880–890.
[125] R.B. Thompson, D. Peterson, W. Mahoney, M. Cramer, B.P. Maliwal, S.W. Suh, C. Frederickson, C. Fierke, P. Herman, Fluorescent zinc indicators for neurobiology, J. Neurosci. Methods 118 (2002) 63–75.
[126] S. Maruyama, K. Kikuchi, T. Hirano, Y. Urano, T. Nagano, A novel, cell-permeable, fluorescent probe for ratiometric imaging of zinc ion, J. Am. Chem. Soc. 124 (2002) 10650–10651.
[127] K. Kiyose, H. Kojima, Y. Urano, T. Nagano, Development of a ratiometric fluorescent zinc ion probe in near-infrared region, based on tricarbocyanine chromophore, J. Am. Chem. Soc. 128 (2006) 6548–6549.

[128] C.J. Chang, J. Jaworski, E.M. Nolan, M. Sheng, S.J. Lippard, A tautomeric zinc sensor for ratiometric fluorescence imaging: Application to nitric oxide-induced release of intracellular zinc, Proc. Natl. Acad. Sci. U. S. A. 101 (2004) 1129–1134.
[129] N.C. Lim, C. Bruckner, DPA-substituted coumarins as chemosensors for zinc(II): modulation of the chemosensory characteristics by variation of the position of the chelate on the coumarin, Chem. Commun. (Camb.) (2004) 1094–1095.
[130] M. Taki, J.L. Wolford, T.V. O'Halloran, Emission ratiometric imaging of intracellular zinc: Design of a benzoxazole fluorescent sensor and its application in two-photon microscopy, J. Am. Chem. Soc. 126 (2004) 712–713.
[131] E. Tomat, S.J. Lippard, Ratiometric and intensity-based zinc sensors built on rhodol and rhodamine platforms, Inorg. Chem. 49 (2010) 9113–9115.
[132] Z.C. Xu, K.H. Baek, H.N. Kim, J.N. Cui, X.H. Qian, D.R. Spring, I. Shin, J. Yoon, Zn(2+)-Triggered Amide Tautomerization Produces a Highly Zn(2+)-Selective, Cell-Permeable, and Ratiometric Fluorescent Sensor, J. Am. Chem. Soc. 132 (2010) 601–610.
[133] T.H. Evers, M.A.M. Appelhof, P.T.H.M. de Graaf-Heuvelmans, E.W. Meijer, M. Merkx, Ratiometric detection of Zn(II) using chelating fluorescent protein chimeras, J. Mol. Biol. 374 (2007) 411–425.